Endoplasmic reticulum-mitochondria miscommunication is an early and causal trigger of hepatic insulin resistance and steatosis

A. Beaulant, M. Dia, B. Pillot, M. A. Chauvin, J. Ji-Cao, C. Durand, N. Bendridi, S. Chanon, A. Vieille-Marchiset, C. C. da Silva, et al.

Research Article
Experimental and Translational Hepatology

JOURNAL
OF HEPATOLOGY

Endoplasmic reticulum-mitochondria miscommunication is an early and causal trigger of hepatic insulin resistance and steatosis

Graphical abstract

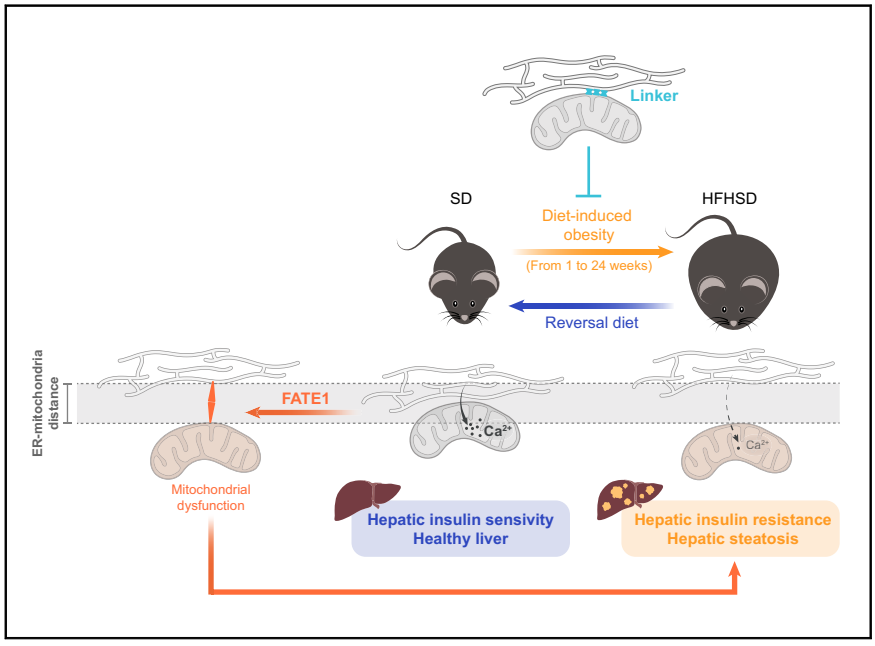

Highlights

- Reduced ER-mitochondria interactions and calcium exchange is an early event in diet-induced obese mice.
- Disrupting ER-mitochondria communication is sufficient to induce hepatic insulin resistance and steatosis.
- Reinforcing ER-mitochondria interactions prevents diet-induced glucose intolerance.
- Switching on a healthy diet concomitantly reverses ER-mitochondria miscommunication and improves hepatic insulin sensitivity.
- ER-mitochondria miscommunication was confirmed in the liver of patients with MAFLD and type 2 diabetes.

Authors

Agathe Beaulant, Maya Dia, Bruno Pillot, …, Ludovic Gomez, Melanie Paillard, Jennifer Rieusset

Correspondence

jennifer.rieusset@univ-lyon1.fr (J. Rieusset).

Lay summary

The literature suggests that interactions between the endoplasmic reticulum and mitochondria could play a role in hepatic insulin resistance and steatosis during chronic obesity. In the present study, we reappraised the time-dependent regulation of hepatic endoplasmic reticulum-mitochondria interactions and calcium exchange, investigating reversibility and causality, in mice with diet-induced obesity. We also assessed the relevance of our findings to humans. We show that organelle miscommunication is an early causal trigger of hepatic insulin resistance and steatosis that can be improved by nutritional strategies.

https://doi.org/10.1016/j.jhep.2022.03.017
 J. Hepatol. 2022, 77, 710–722

Research Article
Experimental and Translational Hepatology

JOURNAL OF HEPATOLOGY

Endoplasmic reticulum-mitochondria miscommunication is an early and causal trigger of hepatic insulin resistance and steatosis

Agathe Beaulant[1], Maya Dia[1], Bruno Pillot[1], Marie-Agnes Chauvin[1], Jingwei Ji-cao[1], Christine Durand[1], Nadia Bendridi[1], Stephanie Chanon[1], Aurelie Vieille-Marchiset[1], Claire Crola Da Silva[1], Stéphanie Patouraux[2,3], Rodolphe Anty[2,3], Antonio Iannelli[2,3], Albert Tran[2,3], Philippe Gual[3], Hubert Vidal[1], Ludovic Gomez[1], Melanie Paillard[1], Jennifer Rieusset[1,*]

[1]*Laboratoire CarMeN, UMR INSERM U1060/INRA U1397, Université Claude Bernard Lyon1, F-69310 Pierre-Bénite and F-69500 Bron, France;* [2]*Université Côte d'Azur, CHU, INSERM, U1065, C3M, Nice, France;* [3]*Université Côte d'Azur, INSERM, U1065, C3M, Nice, France*

Background & Aims: Hepatic insulin resistance in obesity and type 2 diabetes was recently associated with endoplasmic reticulum (ER)-mitochondria miscommunication. These contact sites (mitochondria-associated membranes: MAMs) are highly dynamic and involved in many functions; however, whether MAM dysfunction plays a causal role in hepatic insulin resistance and steatosis is not clear. Thus, we aimed to determine whether and how organelle miscommunication plays a role in the onset and progression of hepatic metabolic impairment.

Methods: We analyzed hepatic ER-mitochondria interactions and calcium exchange in a time-dependent and reversible manner in mice with diet-induced obesity. Additionally, we used recombinant adenovirus to express a specific organelle spacer or linker in mouse livers, to determine the causal impact of MAM dysfunction on hepatic metabolic alterations.

Results: Disruption of ER-mitochondria interactions and calcium exchange is an early event preceding hepatic insulin resistance and steatosis in mice with diet-induced obesity. Interestingly, an 8-week reversal diet concomitantly reversed hepatic organelle miscommunication and insulin resistance in obese mice. Mechanistically, disrupting structural and functional ER-mitochondria interactions through the hepatic overexpression of the organelle spacer FATE1 was sufficient to impair hepatic insulin action and glucose homeostasis. In addition, FATE1-mediated organelle miscommunication disrupted lipid-related mitochondrial oxidative metabolism and induced hepatic steatosis. Conversely, reinforcement of ER-mitochondria interactions through hepatic expression of a synthetic linker prevented diet-induced glucose intolerance after 4 weeks' overnutrition. Importantly, ER-mitochondria miscommunication was confirmed in the liver of obese patients with type 2 diabetes, and correlated with glycemia, HbA1c and HOMA-IR index.

Conclusions: ER-mitochondria miscommunication is an early causal trigger of hepatic insulin resistance and steatosis, and can be reversed by switching to a healthy diet. Thus, targeting MAMs could help to restore metabolic homeostasis.

Lay summary: The literature suggests that interactions between the endoplasmic reticulum and mitochondria could play a role in hepatic insulin resistance and steatosis during chronic obesity. In the present study, we reappraised the time-dependent regulation of hepatic endoplasmic reticulum-mitochondria interactions and calcium exchange, investigating reversibility and causality, in mice with diet-induced obesity. We also assessed the relevance of our findings to humans. We show that organelle miscommunication is an early causal trigger of hepatic insulin resistance and steatosis that can be improved by nutritional strategies.

Introduction

Obesity, type-2 diabetes (T2D) and metabolic dysfunction-associated fatty liver disease (MAFLD) are important metabolic disorders whose incidence is increasing. They are associated with hepatic insulin resistance, which is a major contributor to fasting and postprandial hyperglycemia, and with hepatic lipid accumulation. Therefore, understanding the molecular mechanisms of hepatic insulin resistance and steatosis is crucial for developing new therapeutic strategies to improve whole-body glucose and lipid homeostasis.

Intracellular organelle dysfunction, particularly endoplasmic reticulum (ER) stress and mitochondria alterations, are central to the pathophysiology of hepatic insulin resistance and steatosis.[1] As well as alterations in each organelle, miscommunication recently emerged as a new mechanism of impaired hepatic insulin action[1] and of hepatic lipid accumulation.[2] ER and mitochondria interact at contact sites known as mitochondria-associated membranes (MAMs) or mitochondria-ER contacts, where they exchange phospholipids and calcium (Ca^{2+}), thus modulating key signaling pathways and regulating cellular homeostasis.[3] Notably, we recently identified MAMs as key hubs of nutrient and hormonal signaling in liver,[4,5] skeletal muscle[6] and pancreatic β cells.[7] Importantly, ER-

Keywords: hepatic insulin resistance; hepatic steatosis; mitochondria-associated membranes; calcium signaling; mitochondria oxidative metabolism; lipid oxidation.
Received 9 May 2021; received in revised form 18 February 2022; accepted 7 March 2022; available online 28 March 2022

* Corresponding author. Address: Laboratoire CarMeN, UMR INSERM U1060/INRA U1397 (CarMeN laboratory), Hôpital Lyon Sud - Secteur 2, Bâtiment CENS ELI-2D, 165 Chemin du Grand Revoyet, F - 69310 Pierre Benite, France; Tel.: 33 (0)4 26 23 59 20, Fax: 33 (0)4 26 23 59 16.
E-mail address: jennifer.rieusset@univ-lyon1.fr (J. Rieusset).

https://doi.org/10.1016/j.jhep.2022.03.017

mitochondria communication was impaired in these tissues in various mouse models of obesity and T2D,[4,6] as well as in pancreatic β cells in patients with T2D.[8] In addition, other authors recently demonstrated a strong link between MAM dynamics and lipid homeostasis,[9,10] and that mitofusin 2-related ER-mitochondria miscommunication is associated with hepatic steatosis.[9] However, some authors also found that MAM reinforcement, rather than disruption, was associated with both hepatic[11] and muscular[12] insulin resistance. The reasons for these differences remain unclear, but could be related to the fact i) that MAMs are highly dynamic structures that can be acutely modulated by numerous physiological signals[1] and were shown to be influenced by several physiological and environmental parameters *in vivo*, ii) that MAMs are heterogeneous structures with different thicknesses, each characterized by a specific function,[13] and iii) that MAM proteins are not specific to this interface and may also have other functions outside of MAMs. Therefore, further studies are needed to clearly define the role of MAMs in the control of cellular metabolism, and especially to address the temporal relationship between MAMs and metabolic impairment, to establish MAM structure-function relationships, and to modulate MAMs independently of endogenous proteins, as pointed out in a recent review.[14]

We therefore undertook to reappraise this important issue by combining different mouse models: i) to perform a time-dependent follow-up of the onset of metabolic disorder in a diet-induced mouse model of obesity and MAFLD; ii) to assess the reversibility of the phenotype, using a reversal diet; and iii) to assess *in vivo* modulation of MAMs, using a non-endogenously expressed spacer and linker in the liver of healthy mice and mice with diet-induced obesity. Finally, ER-mitochondria interactions were investigated for the first time in hepatic biopsies from obese patients without or with T2D. This set of approaches led to the conclusion that ER-mitochondria miscommunication observed in mice and humans is an early causal trigger of hepatic insulin resistance and steatosis.

Materials and methods

All material and methods are detailed in the supplementary materials and methods.

Mouse experiments

Mouse studies were performed in accordance with the French Guide for the Care and Use of Laboratory Animals and were approved by the institutional animal research committee of the PBES (ENS, Lyon) and/or the French Ministry (#12658-2017112816023176, 21767-2019082214036668). Nutritional protocols with standard diet (SD) or high-fat high-sucrose diet (HFHSD) and adenoviral infection are described in the supplementary materials and methods. Primary mouse hepatocytes (PMHs) were isolated by 2-step collagenase perfusion via the portal vein.

Human samples

Liver biopsies were obtained during bariatric surgery in obese patients with or without T2D.

ER-mitochondria interactions

ER-mitochondria interactions were analyzed either by *in situ* proximity ligation assay (PLA) or by transmission electronic microscopy (TEM).

Calcium imaging

Measurements of Ca^{2+} were performed at 37°C, using a wide-field Leica DMI6000B microscope equipped with a 40x lens and an ORCA-Flash4.0 digital camera (HAMAMATSU).

Histology

Histologic quantification of hepatic steatosis, inflammation and fibrosis was performed on liver slides.

Insulin signaling and glucose production

Insulin signaling and action were assessed by measuring insulin-stimulated phosphorylation of protein kinase B (PKB) and/or insulin receptor (IR), as well as hepatic glucose production.

Expression analysis

RNA isolation from mouse liver, cDNA synthesis, real-time PCR and protein analysis were performed using standard protocols.

Mitochondrial respiration

Mitochondrial oxygen consumption was measured on either intact or permeabilized PMH (500,000 hepatocytes) using the OROBOROS analyzer at 25°C.

Flow cytometry analysis

Mitochondrial membrane potential and mitochondrial reactive oxygen species (ROS) production were quantified by cytometry.

Statistical analysis

Data are expressed as mean ± SEM. Statistical analyses were performed using GraphPad Prism software and are detailed in the figure legends.

Results

Reduced ER-mitochondria interactions and Ca^{2+} exchange in livers of HFHSD-fed mice precede hepatic insulin resistance and steatosis

We performed a kinetic analysis of MAM structure and function in the liver of mice following 1, 4 ,8, 12 and 16 weeks of SD or HFHSD. Compared to SD mice, HFHSD mice gained more weight (Fig. 1A) and became glucose intolerant (Fig. 1B, Fig. S1A-1E) after as little as 1 week, whereas they developed systemic reduced insulin sensitivity (Fig. 1C-1E, Fig. S1F-1I) and fatty liver (Fig. 1F,G) only after 12 weeks of HFHSD. *In situ* PLA targeting the VDAC1-IP3R1 complex[15] showed that VDAC1-IP3R1 proximity was reduced as early as 1 week after HFHSD, and this reduction was maintained throughout the HFHSD feeding period (Fig. 1H and Fig. S2A-E). We also used TEM to analyze the proportion of mitochondrial membranes in close contact (<50 nm) with the ER, as well as the rate of contacts according to gap width, in liver sections of SD and HFHSD mice after 1 and 16 weeks' diet. We found that an early reduction in organelle interactions after 1 week of HFHSD affected only the closest contacts (0-10 nm) (Fig. 1I, Fig. S3A), whereas all the contacts, ranging from 0 to 50 nm in width, were significantly reduced by 16 weeks' HFHSD (Fig. 1J, Fig. S3B), illustrating progressive worsening of the phenotype during overnutrition. Likewise, the number of contacts per mitochondrion was significantly decreased only after 16 weeks' HFHSD (Fig. S3C). Importantly, diet-induced ER-mitochondria miscommunication was not associated with ER stress in the liver of HFHSD-fed mice (Tables S1 and S2), but mRNA levels of inflammatory and pre-fibrosis markers were increased at the

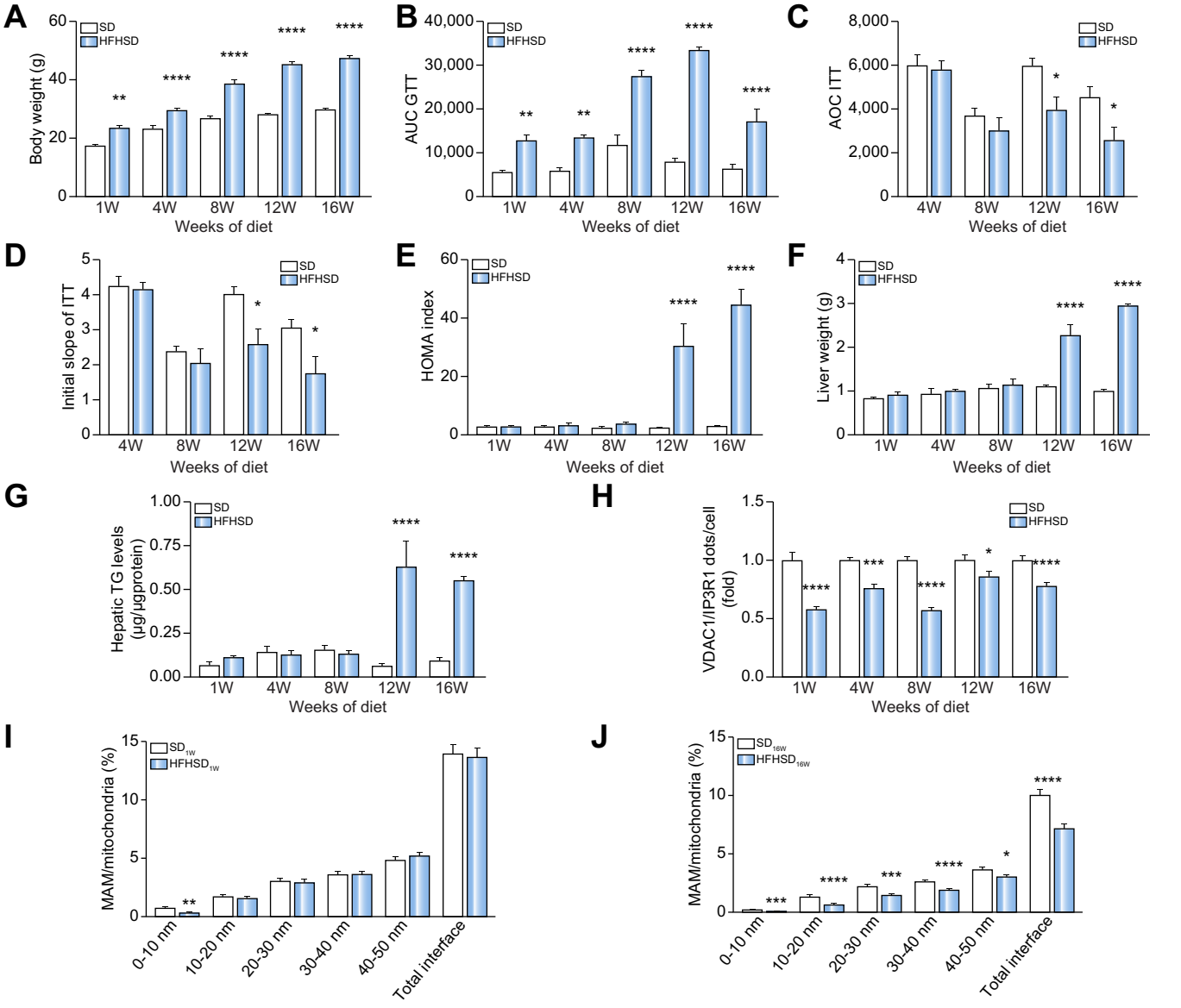

Fig. 1. Disruption of MAMs in the liver of HFHSD-fed mice precedes diet-induced hepatic insulin resistance and steatosis. (A-G) Body weight (A), GTT (B), ITT (C), slope of glucose curves during 0-30 minute ITT (D), HOMA-IR index (E), liver weight (F), and hepatic TG levels (G) in SD- and HFHSD-fed mice from 1 to 16 weeks (n = 3-6 mice/group). H) VDAC1-IP3R1 interactions measured by *in situ* PLA in SD- and HFHSD-fed mouse liver (n = 32-39 images in n = 3 mice/group). (I-J) Structural analysis of ER-mitochondria interactions by TEM in SD and HFHSD mice after 1 week (I) and 16 weeks (J) of feeding. Data are expressed as % MAMs/mitochondria in 50 nm range (total interface) or according to indicated ranges (n = 142-177 mitochondria analyzed in n = 3 mice/group). Sidak's multiple comparison test: *p <0.05; **p <0.01; ***p <0.001; ****p <0.0001 *vs.* SD. AOC, area over the curve; AUC, area under the curve; ER, endoplasmic reticulum; GTT, glucose tolerance test; HFHSD, high-fat and high-sucrose diet; ITT, insulin tolerance test; MAMs, mitochondria-associated membranes; PLA, proximity ligation assay; SD, standard diet; TEM, transmission electronic microscopy.

late stage of HFHSD feeding (Table S1). Taken together, these data demonstrate that structural ER-mitochondria interactions are disrupted early and progressively during diet-induced obesity, long before the onset of insulin resistance and liver steatosis.

Next, we analyzed whether HFHSD-mediated ER-mitochondria miscommunication resulted in MAM dysfunction. As MAMs are key platforms for ER-mitochondria Ca^{2+} exchange,[16] we imaged IP3R-mediated mitochondrial Ca^{2+} accumulation[7] using the FRET-based 4mtD3CPV mitochondrial Ca^{2+} sensor,[17] in SD and HFHSD PMHs. Importantly, we confirmed that $HFHSD_{16W}$ hepatocytes conserved the alterations in both insulin-stimulated PKB phosphorylation (Fig. S4C) and glucose production (Fig. S4F) once isolated and cultured, whereas no alteration was found as expected after 1 and 4 weeks of HFHSD (Figs S4A,B and S4D,E, respectively). As illustrated in Fig. 2A, 1 week's HFHSD significantly reduced ATP-stimulated mitochondrial Ca^{2+} accumulation (at both delta-peak and area under the curve levels: Figs 2C and 2D respectively), whereas basal mitochondrial level was not modified (Fig. 2B). The reduction in ER-mitochondria Ca^{2+} exchange persisted after 4 weeks' HFHSD (Fig. 2E-2H), with no alteration in basal mitochondrial Ca^{2+} levels (Fig. 2F). Consequently, short diet-induced disruption of organelle interactions is associated with reduced

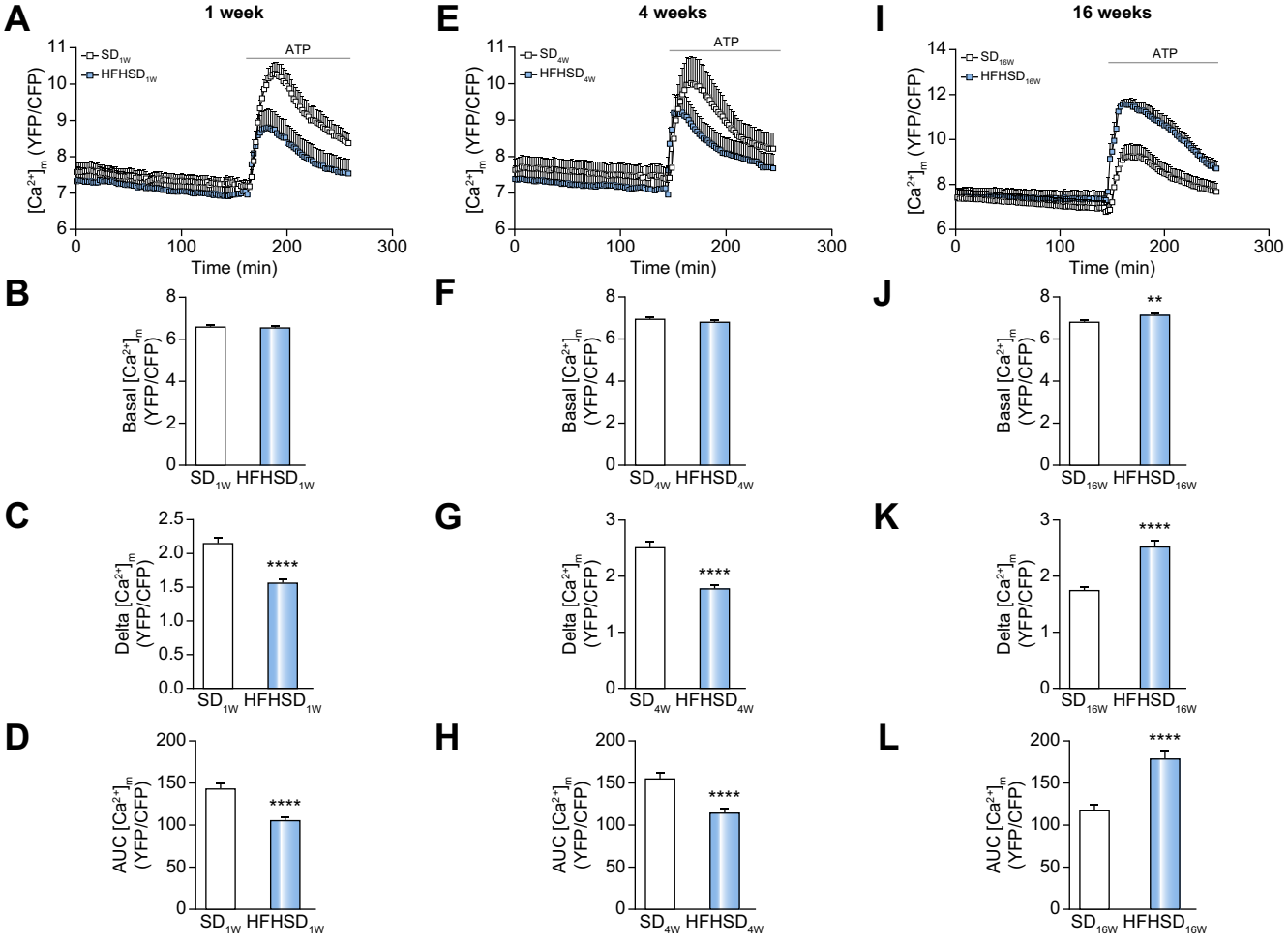

Fig. 2. Early disruption of ER-mitochondria Ca^{2+} exchange in the liver of HFHSD-fed mice. Representative curves from 1 experimental day (A, E, I) and quantitative analysis of basal (B, F, J) and ATP-stimulated (C-D, G-H, K-L) mitochondrial Ca^{2+} accumulation measured in PMHs from SD- and HFHSD-fed mice after 1 week (left column, n = 361-438 cells), 4 weeks (middle column, n = 204-247 cells) and 16 weeks (right column, n = 306-177 cells) of feeding. For ATP-stimulated mitochondrial Ca^{2+} accumulation, both the delta peak (C, G, K) and the AUC (D, H, L) were quantified. Non-parametric Mann-Whitney test: $^{**}p$ <0.01; $^{****}p$ <0.0001 *vs.* respective SD. ER, endoplasmic reticulum; HFHSD, high-fat and high-sucrose diet; PMHs, primary mouse hepatocytes; SD, standard diet.

organelle Ca^{2+} exchange, confirming early ER-mitochondria miscommunication during diet-induced obesity. Surprisingly, after 16 weeks' HFHSD (Fig. 2I), there was a significant increase in mitochondrial Ca^{2+} levels both at the basal level (Fig. 2J) and following ATP stimulation (Fig. 2K,L). This observation led us to postulate that either MAM function is regulated differently from structure after 16 weeks' HFHSD, or that the increase in organelle Ca^{2+} exchange in obese hepatocytes reflects an adaptation process. To address this hypothesis, we measured physical ER-mitochondria interactions by *in situ* PLA in infected hepatocytes of SD_{16W} and $HFHSD_{16W}$ mice, to mimic the conditions of Ca^{2+} measurement. As shown in Fig. S4G, VDAC1-IP3R1 proximity was significantly greater in infected $HFHSD_{16W}$ hepatocytes than in SD_{16W} hepatocytes, suggesting that hepatocyte infection with the mitochondrial Ca^{2+} sensor impaired the MAM phenotype observed *in situ* in the mouse liver. Taken together, these results demonstrate that disrupted ER-mitochondria interactions and Ca^{2+} transfer are an early defect, present after as little as 1 and 4 weeks of overnutrition, and precede diet-induced hepatic insulin resistance and steatosis.

Disruption of ER-mitochondria interactions and calcium exchange is sufficient to alter hepatic insulin sensitivity and induce hepatic steatosis

To experimentally disrupt MAMs in mouse liver, we expressed the organelle spacer FATE1 (fetal and adult testis-expressed 1)[18] using an adenovirus (Ad-FATE1), as previously performed in skeletal muscle.[6] FATE1 efficacy was first validated in cultured PMHs. FATE1 expression reduced VDAC1-IP3R1 proximity, measured by *in situ* PLA, in 36-hour-infected hepatocytes (Fig. 3A). In agreement, ATP-stimulated mitochondrial Ca^{2+} accumulation was significantly reduced in Ad-FATE1 hepatocytes compared to Ad-mCherry hepatocytes (Fig. 3B-3E), confirming FATE1-mediated organelle miscommunication. Surprisingly, basal mitochondrial Ca^{2+} level was increased by acute FATE1 expression (Fig. 3C), suggesting early adaptation of the mitochondrial Ca^{2+} concentration to overcome the acute reduced ER-mitochondria Ca^{2+} transfer. Importantly, this reduction in organelle communication was associated with a reduction in insulin signaling (insulin-stimulated IR and PKB phosphorylation, Fig. 3F-3H) and action

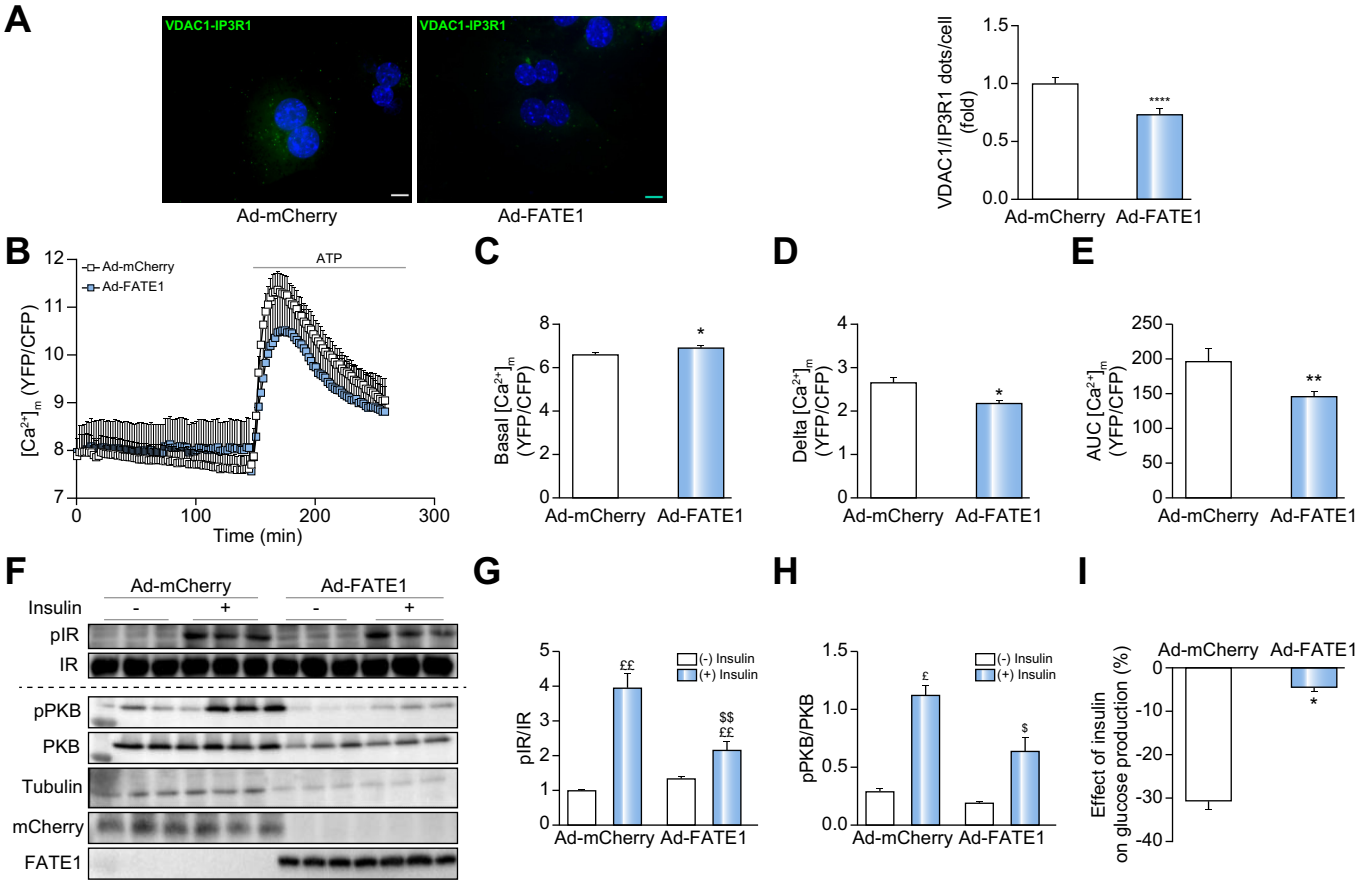

Fig. 3. FATE1-mediated disruption of ER-mitochondria interactions and Ca^{2+} exchange alters insulin signaling in PMHs. (A) Representative images (scale bar = 5 μm) and quantitative analysis of VDAC1-IP3R1 interactions measured by *in situ* PLA in infected hepatocytes (n = 84-116 images from n = 4 independent experiments). B-E) Representative curves (B) and quantitative analysis of basal (C) and ATP-stimulated (D-E) mitochondrial [Ca^{2+}] in infected hepatocytes (n = 181-203 cells analyzed in n = 5 independent experiments). F-H) Representative western blot (F) and quantitative analysis of insulin-stimulated IR (H) and AKT (G) phosphorylation in infected hepatocytes (triplicate in n = 4 mice/group). Note that analyses of IR and PKB phosphorylation were not performed on the same samples (separated by a dotted line) and that total AKT/tubulin ratio is not modified by FATE1 expression when all gels are combined. (I) Effect of insulin on glucose production measured in PMHs from infected mice (n = 4 mice/group). Non-parametric Mann-Whitney test: $^{*}p$ <0.05; $^{**}p$ <0.01; $^{****}p$ <0.0001 *vs.* Ad-mCherry, $^{£}p$ <0.05; $^{££}p$ <0.01 *vs.* (-) insulin, $^{\$}p$ <0.05; $^{\$\$}p$ <0.01 *vs.* (+) insulin. ER, endoplasmic reticulum; PLA, proximity ligation assay; PMHs, primary mouse hepatocytes. (This figure appears in color on the web.)

(inhibitory effect of insulin on glucose production, Fig. 3J), suggesting that acute FATE1-related MAM disruption could alter hepatic insulin sensitivity.

Subsequently, the effect of FATE1 was investigated *in vivo*, after infection of 12-week-old male C57BL/6 mice with either Ad-mCherry (as control) or Ad-FATE1. Two weeks later, around 50% of hepatocytes were infected in infected mice (Fig. S5A). FATE1 expression was specific to the liver, as it was not found in either skeletal muscle or adipose tissue (Fig. S5B). Liver subcellular fractionation confirmed that FATE1 was well targeted to the ER and present in MAM fractions, whereas it was not found in pure mitochondria fractions (Fig. S5C). Importantly, FATE1 expression resulted in reduced VDAC1-IP3R1 proximity (Fig. 4A) and in a reduced proportion of mitochondrial membranes in close contact with ER (0-10 and 10-20 nm, Fig. 4B), without changing ER or mitochondria contacts with lipid droplets (LDs) (Fig. S5D-5E). Hepatocytes from Ad-mCherry and Ad-FATE1 mice were isolated to measure mitochondrial Ca^{2+} levels. As illustrated in Fig. 4C, chronic FATE1 expression significantly reduced both basal (Fig. 4D) and ATP-stimulated (Fig. 4E-4F) mitochondrial Ca^{2+} accumulation. Taken together, these data demonstrate that, as expected, *in vivo* FATE1 overexpression disrupted both organelle interactions and Ca^{2+} exchange in the mouse liver.

Next, we investigated repercussions on metabolic homeostasis. Ad-FATE1 mice had similar body weight (25.2±0.57 g *vs.* 23.9±0.52 g, n = 10 mice/group, n.s.) and liver weight (1.26±0.07 g *vs.* 1.5±0.11 g, n = 10 mice/group, ns) to Ad-mCherry mice. Ad-FATE1 mice showed significant hyperglycemia after 6 hours' fasting (Fig. 5A), and glucose intolerance on glucose tolerance test (Fig. 5B,C), while systemic insulin sensitivity during the insulin tolerance test was not modified by hepatic overexpression of FATE1 (Fig. 5D-G). However, analysis of hepatic insulin sensitivity revealed reduced insulin-stimulated phosphorylation of both IR and PKB in the liver of Ad-FATE1 mice (Fig. 5H,I). Additionally, insulin-mediated inhibition of glucose production was dampened in chronic Ad-FATE1 *vs.* Ad-mCherry PMHs (Fig. 5J). Lastly, investigation of hepatic injury found no effect of FATE1 expression on hepatic ER stress (Tables S3-4), inflammation (Fig. S6A,B) or fibrosis (Fig. S6A,C). However, chronic FATE1 expression induced hepatic steatosis, with a significant increase in both LD content and size (Fig. 5K-M), corresponding to microsteatosis, as the majority of LDs (30%) are around 0.5-1 μm^2

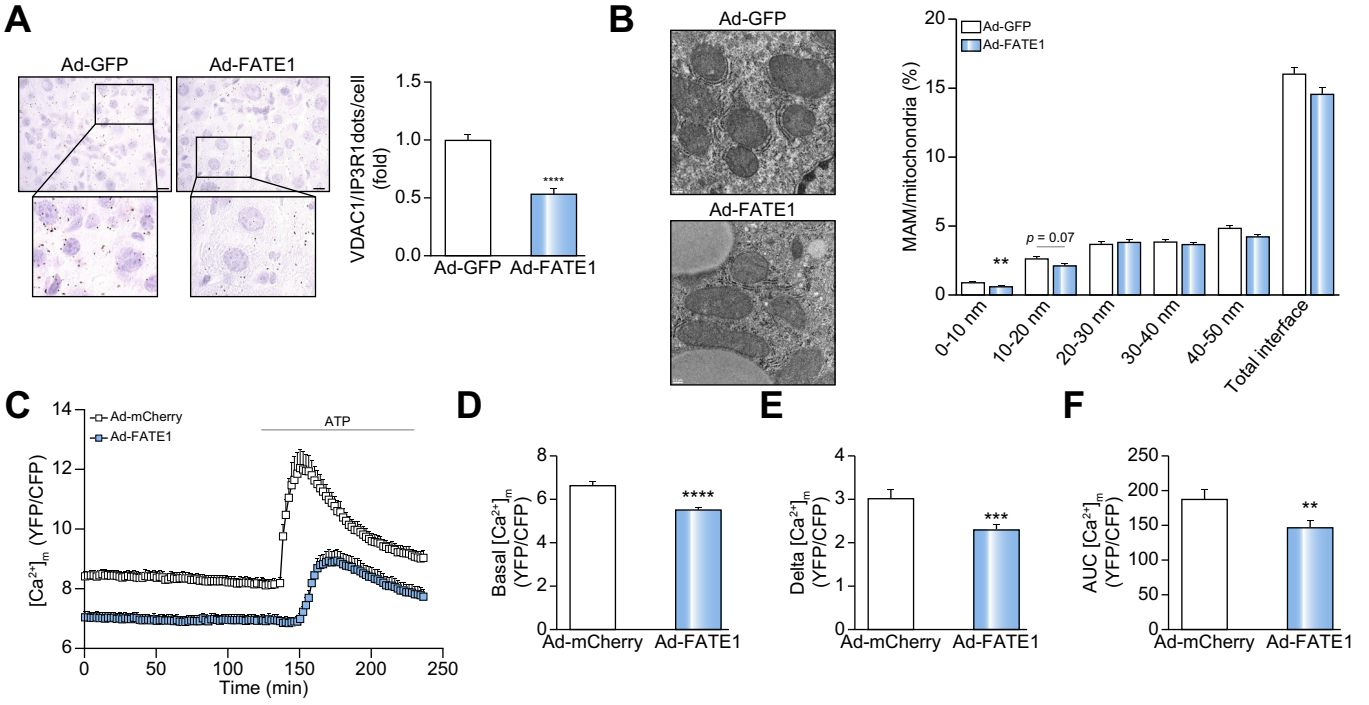

Fig. 4. Hepatic FATE1 expression disrupts ER-mitochondria interactions and Ca^{2+} exchange in healthy mice. A) Representative images (scale = 10 μm) and quantitative analysis of VDAC1-IP3R1 interactions measured by *in situ* PLA in the liver of infected mice (n = 88-99 images analyzed from n = 9-10 mice/group). (B) Representative TEM images (scale bar = 0.2 μm) and quantitative analysis of ER-mitochondria interactions in the liver of infected mice. Data are expressed as % MAMs/mitochondria in 50 nm range (total interface) or according to indicated range (n = 645-519 mitochondria analyzed in n = 10 mice/group). (C-F) Representative curves (C) and quantitative analysis of basal (D) and ATP-stimulated (E-F) mitochondrial [Ca^{2+}] in infected hepatocytes (n = 45-94 cells analyzed in n = 3 mice/group). Non-parametric Mann-Whitney test: $^{**}p$ <0.01; $^{***}p$ <0.001; $^{****}p$ <0.0001 *vs.* Ad-GFP/Ad-mCherry. ER, endoplasmic reticulum; MAMs, mitochondria-associated membranes; PLA, proximity ligation assay. (This figure appears in color on the web.)

and the nucleus is centrally located (Fig. S6D). In addition, triglyceride levels were also increased in Ad-FATE1 liver (Fig. 5N), without modification of mRNA levels of key genes of lipid metabolism (Fig. S6E). Taken together, these data demonstrate that FATE1-mediated organelle miscommunication alters hepatic insulin sensitivity and glucose homeostasis and induces hepatic steatosis.

Hepatic steatosis in Ad-FATE1 mice could be linked to reduced mitochondrial lipid oxidation secondary to organelle miscommunication. Therefore, we measured palmitate-linked mitochondrial oxygen consumption in intact hepatocytes of Ad-mCherry and Ad-FATE1 mice (Fig. S7A). As shown in Fig. 5O, FATE1 overexpression significantly reduced both basal and maximal FCCP (carbonylcyanide-4-trifluoromethoxyphenylhydrazone)-induced mitochondrial respiration under palmitate. Incubation of hepatocytes with etomoxir, an inhibitor of lipid oxidation, prevented FCCP-induced mitochondrial respiration in both Ad-mCherry and Ad-FATE1 PMHs. However, both basal and maximal respiration were still lower in the presence of etomoxir in Ad-FATE1 PMHs (Fig. 5P), suggesting potential additional intrinsic mitochondrial dysfunction. Therefore, we measured mitochondrial respiration in permeabilized hepatocytes in the presence of complex substrates (Fig. S7B). As shown in Fig. S7C, basal mitochondria oxygen consumption was not modified by FATE1 expression, but maximal respiration in response to complex II and IV activation was significantly lower in Ad-FATE1 permeabilized hepatocytes, whereas the reduction was not significant in complex I substrates. These effects were independent of change in mitochondrial density (Fig. S7D), mitochondrial membrane potential (Fig. S7E) and mitochondrial ROS production (Fig. S7F). Taken together, these data suggest that FATE1-mediated hepatic steatosis could be linked to both reduced mitochondrial lipid oxidation and intrinsic mitochondrial dysfunction.

Reinforcement of MAMs prevents HFHSD-induced glucose intolerance in mice

To reinforce organelle communication, we used a previously developed organelle linker[19] after validation in PMHs. As shown in Fig. 6A, 36 hours' adenovirus-mediated expression of the linker (Ad-Linker) increased ATP-stimulated mitochondrial Ca^{2+} accumulation (Fig. 6C-D), without modifying basal mitochondrial Ca^{2+} levels (Fig. 6B). Interestingly, the Ad-linker effect was associated with improvement in the palmitate-induced alterations of insulin-stimulated PKB phosphorylation (Fig. 6E), suggesting that reinforcing ER-mitochondria communication improves hepatic insulin sensitivity. To assess this effect *in vivo*, we infected mice by retro-orbital injection of Ad-Ctrl/Ad-linker and consecutively challenged them with HFHSD for 4 weeks. HFHSD duration in this preventive protocol was chosen to maintain hepatic overexpression of the linker and because 4 weeks' HFHSD was sufficient to disrupt organelle communication (Fig. 1). We confirmed that hepatocyte infection persisted after 1 month's feeding with adenovirus (Fig. S8A). Analysis of ER-mitochondria interactions by TEM showed that the linker significantly increased physical connections between organelles in both SD- and HFHSD-fed mice (Fig. 6F, Fig. S8B), and even prevented HFHSD-induced organelle miscommunication (Fig. 6F, Fig. S8B). As shown in Fig. 6G,

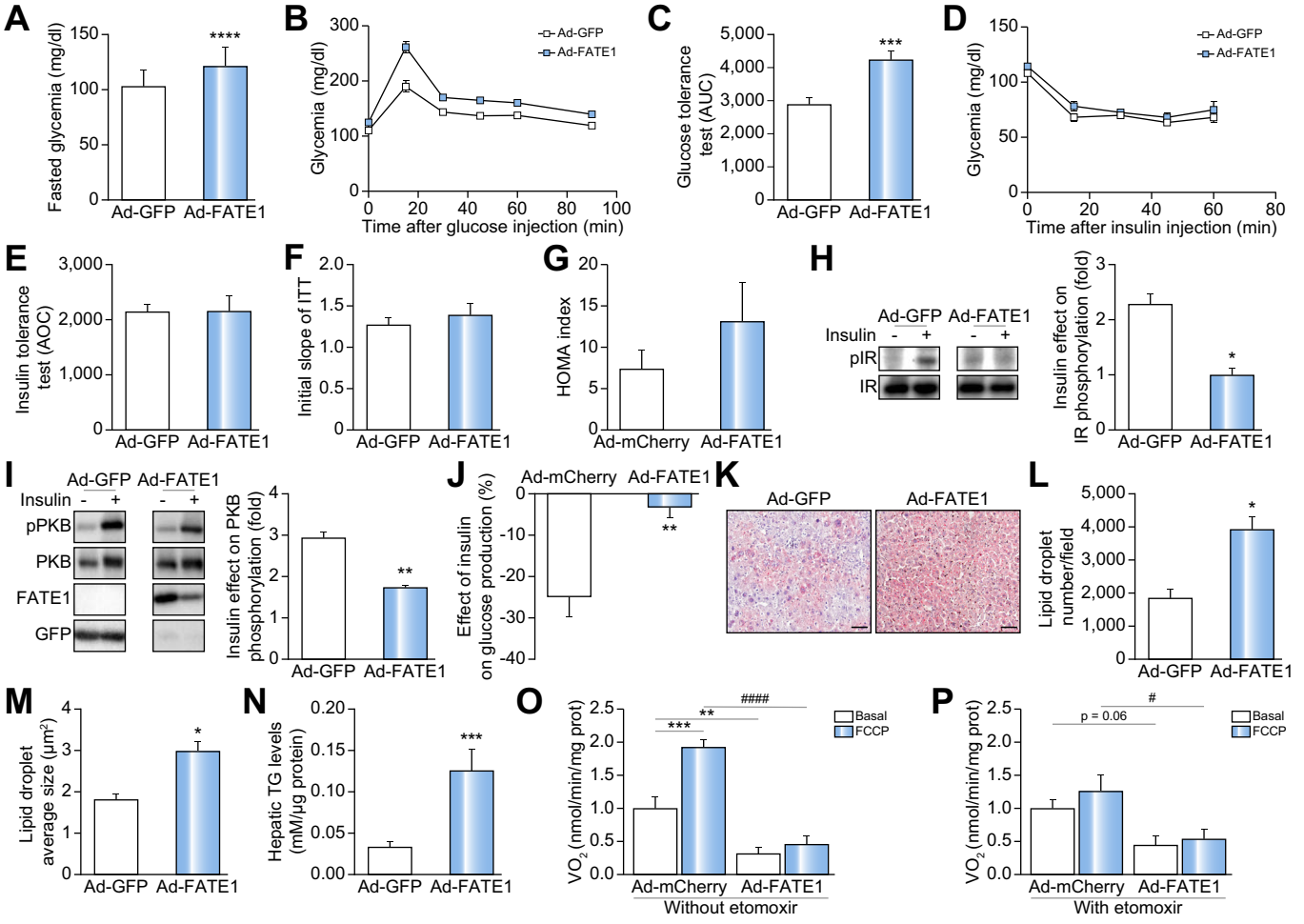

Fig. 5. FATE1-mediated hepatic disruption of organelle communication dampens hepatic insulin sensitivity and induces microsteatosis in healthy mice. (A-B) Average curves of glycemia during GTT (A: n = 30-32 mice/group) and ITT (B: n = 10-14 mice/group) in infected mice. (C-G) Quantitative analysis of 6 hour fasting glycemia (C), AUC during GTT (D), AOC during ITT (E), slope of glucose curves during 0–30-minute ITT (F), HOMA-IR index (G) in infected mice. (H-I) Representative western blot and quantitative analysis of insulin's effect on IR (H) and PKB (I) phosphorylation in the liver of infected mice (n = 3 mice/group). (J) Effect of insulin on hepatic glucose production measured in PMHs from infected mice (n = 6 mice/group). (K-M) Representative images (K) and quantitative analysis of LD content (L) and size (M) in infected mice, measured by oil red O staining (image scale = 100 μM, n = 14 mice/group). (N) triglycerides in the liver of infected mice (n = 14 mice/group). (O-P) Basal and maximal FCCP-induced mitochondrial oxygen consumption was measured either in intact hepatocytes under palmitate in the absence (O) or presence (P) of etomoxir, an inhibitor of lipid oxidation (n = 6 mice/group). (A-N) Non-parametric Mann-Whitney test: $^{*}p$ <0.05; $^{**}p$ <0.01; $^{***}p$ <0.001; $^{****}p$ <0.0001 *vs.* Ad-GFP. (O-P) Sidak's multiple comparison test: $^{*}p$ <0.05, $^{**}p$ <0.01, $^{***}p$ <0.001 *vs.* respective Ad-mCherry, $^{\#}p$ <0.05, $^{\#\#\#\#}p$ <0.0001 *vs.* Ad-mCherry FCCP. AOC, area over the curve; AUC, area under the curve; FCCP, carbonylcyanide-4-trifluoromethoxyphenylhydrazone; GTT, glucose tolerance test; ITT, insulin tolerance test; LD, lipid droplet; PMHs, primary mouse hepatocytes. (This figure appears in color on the web.)

linker expression in SD_{4W} mice did not affect the glucose tolerance test, but markedly improved $HFHSD_{4W}$-induced glucose intolerance. We further analyzed hepatic insulin sensitivity (Fig. S8C), steatosis (Fig. S9A), inflammation (Fig. S9B) and fibrosis (Fig. S9C) in infected mice. However, as 4 weeks' HFHSD was not sufficient to alter insulin sensitivity and induce hepatic injury, we did not find any beneficial effects of the linker on these parameters.

We further analyzed the effects of the linker on lipid-related mitochondrial respiration. Linker expression tended to increase both basal and maximal FCCP-induced mitochondrial respiration under palmitate, in both SD_{4W} and $HFHSD_{4W}$ hepatocytes compared to Ad-Ctrl cells (Fig. 6H). However, $HFHSD_{4W}$ did not alter palmitate-related mitochondrial respiration compared to SD_{4W}. Interestingly, linker expression reduced the number of LDs in both SD_{4W} and $HFHSD_{4W}$ hepatocytes, becoming significant only after HFHSD feeding (Fig. 6I).

Switching to a healthy diet reverses ER-mitochondria miscommunication and improves hepatic insulin sensitivity and steatosis

As MAMs control glucose homeostasis, we then tested the reversibility of the phenotype by switching the $HFHSD_{16W}$ mice to SD for either 4 or 8 additional weeks ($HFHSD_{16W}$+$RD_{4W/8W}$), whereas a group of control mice were kept on either SD or HFSHD ($SD_{20W/24W}$ and $HFSHD_{20W/24W}$, respectively). Four weeks' reversal diet (RD_{4W}) was sufficient to partially improve body weight, fasting glycemia, glucose intolerance and hepatic steatosis compared to $HFHSD_{20W}$ mice (Fig. 7A-7D). However, neither systemic nor hepatic insulin resistance were significantly improved by RD_{4W} (Fig. 7E and 7F). Importantly, a longer reversal diet (RD_{8W}) maintained the phenotype (Fig. 7H-K), and further improved systemic (Fig. 7L, Fig. S10A,B) and hepatic (Fig. 7M) insulin sensitivity. Likewise, the inhibitory effect of insulin on glucose production by PMHs was also improved by RD_{8W}

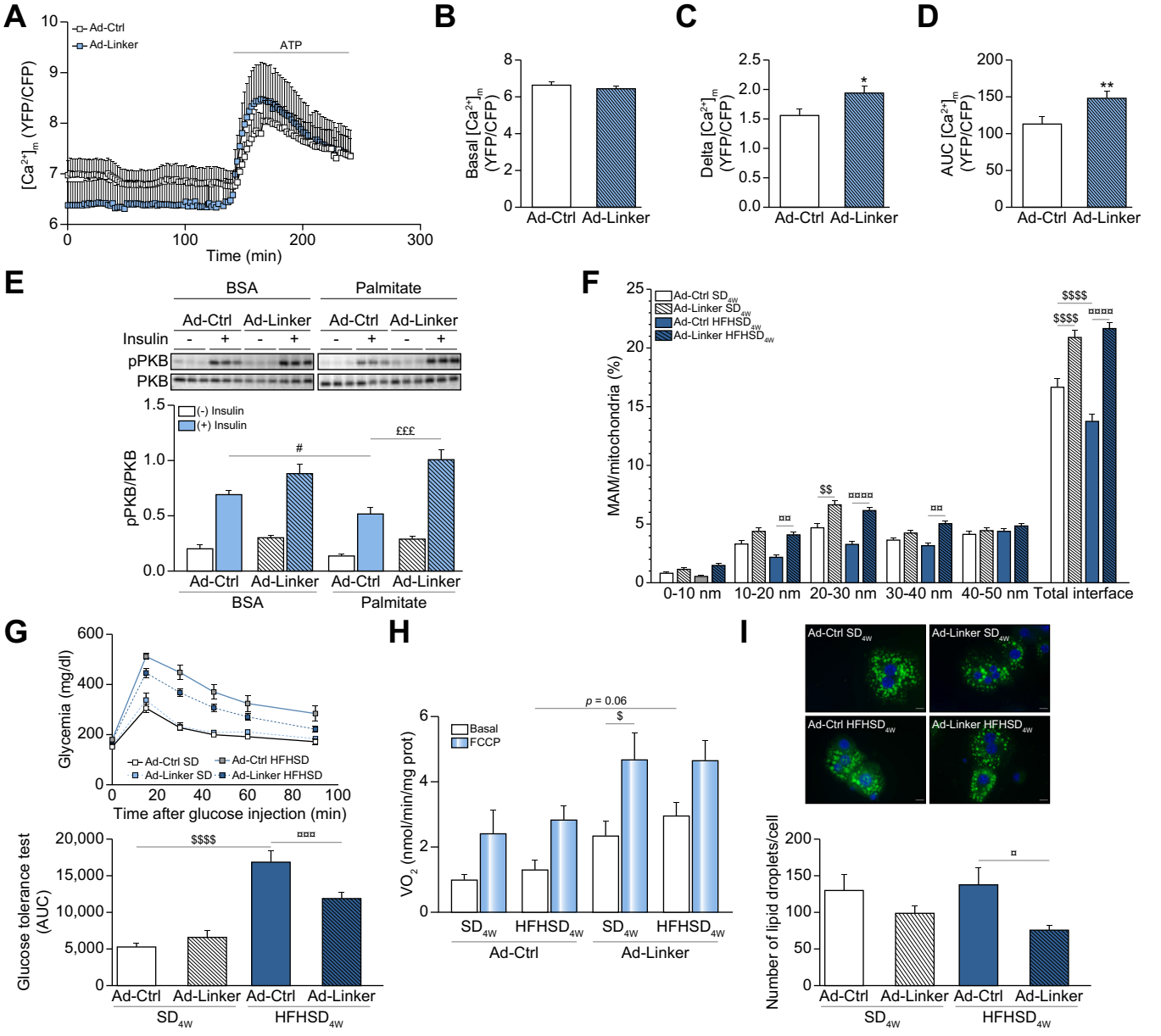

Fig. 6. Linker-mediated reinforcement of hepatic ER-mitochondria interactions and Ca^{2+} transfer prevents diet-induced glucose intolerance in HFHSD-fed mice. (A-D) Representative curves (A) and quantitative analysis of basal (B) and ATP-stimulated (C-D) mitochondrial [Ca^{2+}] in infected hepatocytes (n = 69-73 cells analyzed in n = 4 independent experiments; non-parametric Mann-Whitney test). (E) Analysis of insulin-stimulated PKB phosphorylation in isolated hepatocytes infected for 48 hours with Ad-Ctrl and Ad-linker (n = 2 independent experiments in triplicate, Sidak's multiple comparison test). Blots from BSA and palmitate-treated samples were processed in parallel. (F-J) Mice were infected with Ad-GFP (as control) or Ad-FATE1 and fed with either SD or HFHSD for 4 weeks. (F) ER-mitochondria interactions measured by TEM in the livers of infected mice. Data are expressed as % MAMs/mitochondria in 50 nm range (total interface) or according to indicated ranges (n = 249-441 mitochondria analyzed in n = 5 mice/group, Sidak's multiple comparison test). (G) Average curve of glycemia (at top) and quantitative analysis of AUC (at bottom) during GTT performed in infected mice (n = 10 mice/group, Sidak's multiple comparison test). (H) Basal and FCCP-stimulated mitochondrial oxygen consumption measured in PMHs from infected mice (n = 5 mice/group, Sidak's multiple comparison test). (I) Representative images (scale bar = 10 μm) and quantitative analysis of LD number in BODIPY-labelled infected hepatocytes (n = 5 mice/group, Sidak's multiple comparison test). $^{*}p$ <0,05, $^{**}p$ <0,01 *vs.* Ad-Ctrl; $^{\#}p$ <0,05 *vs.* Ad-Ctrl-BSA(+) insulin; $^{£££}p$ <0,001 *vs.* Ad-Ctrl palmitate (+) insulin; ¤¤p <0.01, ¤¤¤p <0.001, ¤¤¤¤p <0.0001 *vs.* Ad-Ctrl $HFHSD_{4W}$; $^{\$\$}p$ <0,0001, $^{\$\$\$\$}p$ <0.0001 *vs.* Ad-Ctrl SD_{4W}. ER, endoplasmic reticulum; FCCP, carbonylcyanide-4-trifluoromethoxyphenylhydrazone; GTT, glucose tolerance test; HFHSD, high-fat and high-sucrose diet; ITT, insulin tolerance test; LD, lipid droplet; MAMs, mitochondria-associated membranes; PMHs, primary mouse hepatocytes; SD, standard diet; TEM, transmission electron microscopy. (This figure appears in color on the web.)

(Fig. S10C), confirming that longer RD efficiently improved hepatic insulin sensitivity. Then, we analyzed hepatic ER-mitochondria interactions in all mouse groups by *in situ* PLA. We confirmed reduced VDAC1-IP3R1 proximity in both $HFHSD_{20W}$ and $HFHSD_{24W}$ mice compared to their respective SD mice (Fig. 7G and 7N). Importantly, only RD_{8W} restored ER-mitochondria communication in the liver (Fig. 7N), confirming the tight relationship between organelle interactions and hepatic insulin sensitivity. Taken together, these data demonstrate that HFHSD-induced organelle miscommunication can be reversed by a normal diet and is regulated mirror-wise to systemic and hepatic insulin sensitivity.

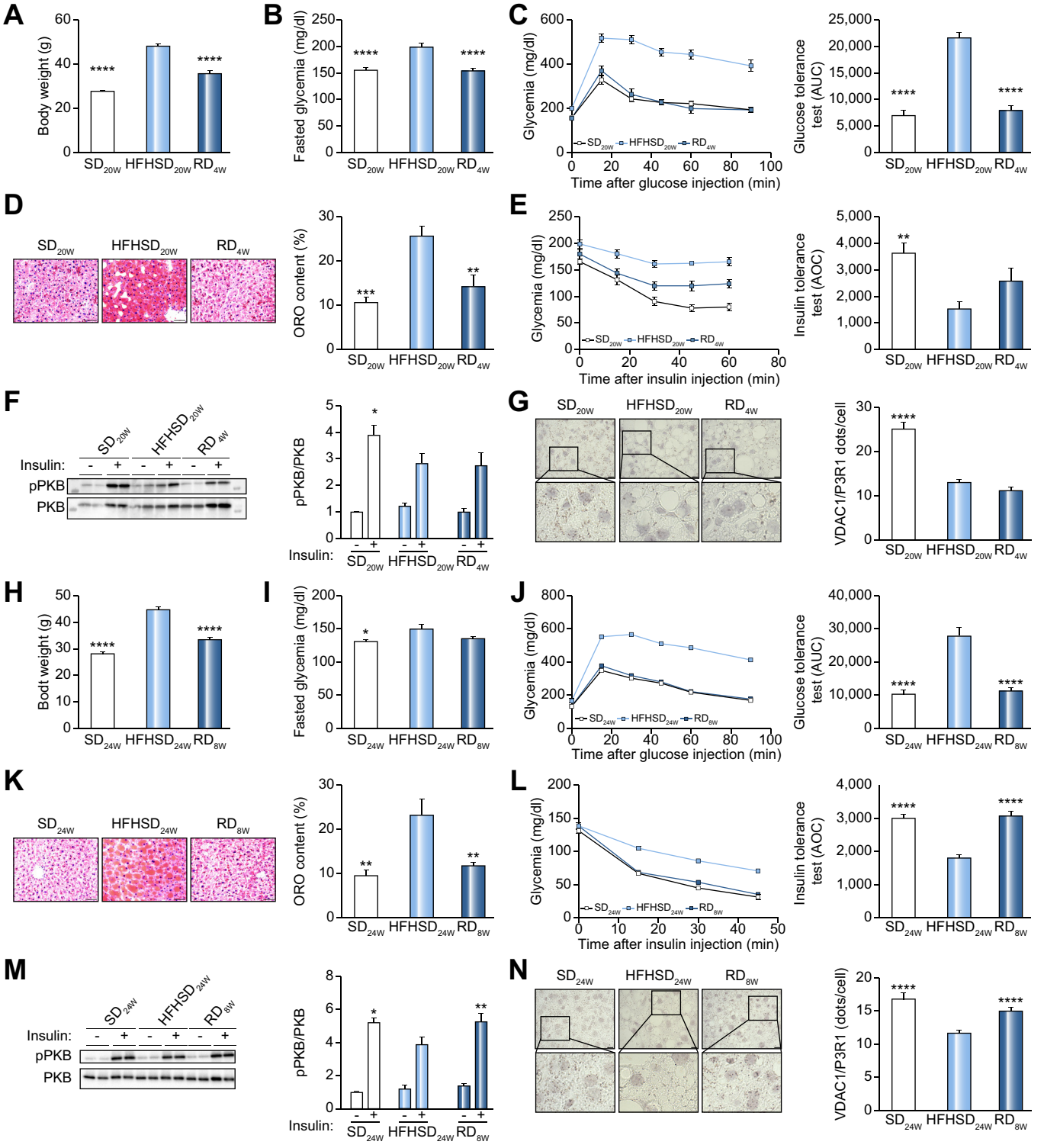

Fig. 7. Hepatic ER-mitochondria miscommunication in HFHSD-fed mice is reversible by switching to healthy diet. Mice were fed with either SD or HFHSD for 16 weeks, and then half of the HFHSD-fed mice were switched to SD for 4 (A-G, RD_{4W}, n = 11-12 mice/group) or 8 (H-N, RD_{8W}, n = 13-14 mice/group except for GTT n = 6 mice/group) additional weeks. Body weight (A, H), fasted glycemia (B, I), GTT (C, J), hepatic lipid accumulation (D, K, N= 4 mice/group), ITT (E, L), insulin-mediated PKB phosphorylation (F, M, n = 4 mice/group) and VDAC1-IP3R1 interactions (G, n = 23-40 images on n = 3-4 mice/group; N, n = 36-38 images on n = 4 mice/group) of SD, HFHSD and RD mice after 4 (A-G) and 8 (H-N) weeks of RD. Sidak's multiple comparison test: $^{*}p$ <0.05; $^{**}p$ <0.01; $^{***}p$ <0.001; $^{****}p$ <0.0001 *vs.* respective HFHSD. ER, endoplasmic reticulum; GTT, glucose tolerance test; HFHSD, high-fat and high-sucrose diet; ITT, insulin tolerance test; RD, reversal diet; SD, standard diet. (This figure appears in color on the web.)

Reduced ER-mitochondria interactions in the liver of patients with T2D

To evaluate the relevance of MAMs in human pathology, we next examined the relationship between hepatic ER-mitochondria interactions and insulin resistance in human liver biopsies from obese patients. Patients were dichotomized based on the presence or absence of T2D (Fig. 8A). Hepatic steatosis grade on histology did not differ between the 2 groups (Fig. 8A). Importantly, hepatic VDAC1-IP3R1 interactions quantified by *in situ* PLA were significantly lower in obese patients with than without T2D (Fig. 8B). In addition, organelle communication correlated negatively with fasting glycemia (Fig. 8C), HbA1c levels (Fig. 8D) and HOMA-IR index (Fig. 8E), indicating that ER-mitochondria communication could be a marker of insulin sensitivity in humans.

Discussion

The dynamic nature of MAMs and the lack of kinetic studies probably contributed to some controversial interpretations regarding the link between ER-mitochondria miscommunication and hepatic insulin resistance in mouse models of chronic obesity and T2D.[4,11] The novelty of the present study was to better understand time-dependent MAM regulation during diet-induced obesity and insulin resistance and its reversibility, and to determine the causal impact of MAM dysfunction on hepatic metabolic alterations by expressing specific organelle spacers or linkers in mouse livers, using recombinant adenovirus. Taken together, our data clearly demonstrated that the reduction in both ER-mitochondria interactions and Ca^{2+} exchange in mouse liver is an early, causal and reversible trigger of hepatic insulin resistance and steatosis. Importantly, MAM disruption was demonstrated for the first time in liver biopsies of obese patients with T2D.

We performed a substantial and careful analysis, combining several complementary imaging and metabolic approaches in PMHs and mouse liver, in order to decipher the regulation of MAM structure and function in relation to diet-induced hepatic insulin resistance and steatosis. Combining a kinetic study and reverse diet protocol enabled extensive analysis of organelle communication from 1 to 24 weeks' HFHSD feeding. Whereas obesity and glucose intolerance appeared early under HFHSD,

A

Characteristics of the obese patients			
	Without T2D	With T2D	*p*
n	21	11	
Gender (F/M)	(21/0)	(11/0)	
Age (years)	39.2 ± 12.7	48.3 ± 8.2	0.0495
BMI (kg/m²)	41.6 ± 3.4	45.0 ± 5.8	0.0978
ALT (IU/L)	34.0 ± 19.2	25.8 ± 9.7	0.2018
AST (IU/L)	26.9 ± 9.9	24.0 ± 7.2	0.4384
Fasting insulin (mIU/L)	16.8 ± 7.2	20.1 ± 7.3	0.1520
Fasting glucose (mmol/L)	4.5 ± 0.7	5.3 ± 0.5	<0.0001
HOMA-IR	3.4 ± 1.5	6.7 ± 3.3	0.0010
HbA1c (%)	5.5 ± 0.3	6.7 ± 1.5	<0.0001
NAFLD activity score	1.9 ± 0.9	2.0 ± 0.8	0.9447
Grade of steatosis	1.9 ± 0.9	2.0 ± 0.8	0.9447

Without T2D: patients without type 2 diabetes; with T2D: patients with type 2 diabetes;
data are expressed as mean ± SD and compared using the non parametric Mann Whitney test

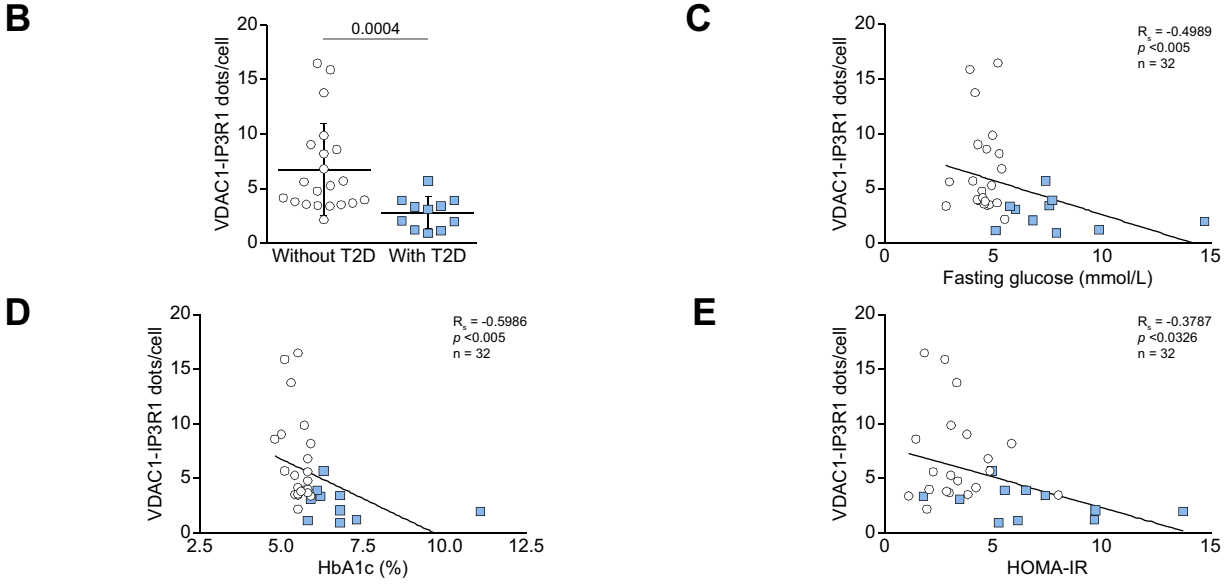

Fig. 8. T2D is associated with decreased hepatic ER-mitochondria interactions in obese patients. (A) Characteristics of obese patients with or without T2D. (B) Quantitative analysis of ER-mitochondria interactions measured by *in situ* PLA in the liver of obese patients with (n = 11) or without T2D (n = 21). Results are expressed as mean ± SD and statistically analyzed on Mann-Whitney test: $^{**}p$ <0.005, $^{***}p$ <0.0005. (C-E) Correlations between ER-mitochondria interactions and fasting glycemia (C), HbA1c levels (D) or HOMA-IR index (E) were analyzed using Spearman's correlation test. ER, endoplasmic reticulum; PLA, proximity ligation assay; T2D, type 2 diabetes.

reduced systemic and hepatic insulin sensitivity, as well as hepatic injuries (steatosis, inflammation and pre-fibrosis) were observed only after 12 weeks' overnutrition. Surprisingly, hepatic ER stress was not present in this nutritional model of MAFLD, likely as a consequence of the HFHSD (only 35% of lipids provided by soybean oil, mostly composed of polyunsaturated fatty acids) or the nutritional status of the mice (sacrifice after overnight fasting, which could have dampened ER stress). Nevertheless, all our data in this model clearly highlighted the occurrence of ER-mitochondria miscommunication ahead of gradual diet-induced metabolic alterations. Using *in situ* PLA and/or TEM, we found that ER-mitochondria contact sites were consistently reduced *in situ* in the liver of HFHSD-fed mice after as little as 1 week and up to 24 weeks' HFHSD feeding. Notably, PLA and TEM analyses showed different amplitudes of ER-mitochondria miscommunication under HFHSD, because i) they provided different information (number of contacts with TEM, and proximity between 2 partners of the functional channeling calcium complex with PLA), ii) they were calculated differently (normalization by mitochondria in TEM, and not in PLA), and iii) they are differentially impacted by the increased cell size in fatty liver (PLA being more strongly impacted than TEM). Nevertheless, we confirmed our previous observations that ER-mitochondria interactions are disrupted in PMHs of $HFHSD_{16W}$ mice compared to SD_{16W} hepatocytes.[4] The use of these 2 complementary methods further suggests that early HFHSD-induced disruption of MAMs is restricted to the closest contacts (0-10 nm) and is rather specific to VDAC1-IP3R1 calcium coupling, whereas the structural alterations after longer overnutrition are more generalized, affecting all gap widths between 0 and 50 nm. Importantly, we demonstrated for the first time that ER-mitochondria Ca^{2+} exchange was also reduced after as little as 1 and 4 weeks' HFHSD, identifying MAM dysfunction as an early alteration during HFHSD feeding. These data are in agreement with our previous observations that altered Ca^{2+} transfer from ER to mitochondria linked alterations of MAM integrity to hepatic insulin resistance in cyclophilin D knockout mice.[20] However, we also found that ER-mitochondria Ca^{2+} exchange was increased in $HFHSD_{16W}$ hepatocytes despite reduced contact in $HFHSD_{16W}$ liver. The larger number of ER-mitochondria interactions in $HFHSD_{16W}$ than SD_{16W} hepatocytes following infection with the mitochondrial Ca^{2+} probe, contrary to *in situ* findings in the liver of obese mice, suggests that *in vitro* use of adenovirus may have impacted organelle communication in $HFHSD_{16W}$ hepatocytes, which are characterized by dysfunctional stressed mitochondria,[21] leading to elevated Ca^{2+}. This experimental condition was apparently without consequences for $HFHSD_{1w}$ or $HFHSD_{4W}$ hepatocytes, likely because mitochondria are more functional in early stages of overnutrition.[22] However, it cannot be excluded that increasing Ca^{2+} transfer with chronic obesity could be a long-term adaptive process to compensate for the reduce number of organelle contact sites, as mitochondrial Ca^{2+} overload was previously found in *ob/ob* hepatocytes compared to lean controls.[11] However, in that study, the authors analyzed MAMs in adenovirus-infected lean and obese mice, and the observed reinforcement of organelle contacts may have resulted from an adenovirus-linked response, as observed in the present study. We were therefore not able to draw any conclusions regarding ER-mitochondria Ca^{2+} exchange in chronic obesity, due to these inherent experimental limitations. Genetic mouse models constitutionally overexpressing the mitochondrial Ca^{2+} probe will be required to settle this question. Even so, our data clearly demonstrated that reduced ER-mitochondria interactions and Ca^{2+} exchange are early defects during overfeeding, preceding altered hepatic insulin sensitivity and hepatic steatosis, thus identifying ER-mitochondria miscommunication as a possible cause of these metabolic alterations.

To confirm this assumption, we experimentally modulated hepatic ER-mitochondria communication using an adenoviral strategy. We took care to study lean mice, to overcome the limitation of this experimental approach with obese mice described above. Importantly, we chose to modulate organelle communication using non-endogenously expressed spacer and linker proteins, as endogenous MAM proteins can have pleiotropic effects outside of MAMs. Modulation of endogenous MAM proteins led to different metabolic phenotypes in mice, as loss of cyclophin D[20] or mitofusin 2[23] induced hepatic insulin resistance and steatosis, whereas downregulation of IP3R1 and PACS2 improved glucose intolerance in obese mice.[11] Therefore, we used FATE1, which has been reported to be an organelle spacer protein.[18] We previously confirmed that FATE1 expression in mouse skeletal muscle reduced ER-mitochondria interactions and altered insulin signaling.[6] Here, we demonstrated that hepatic FATE1 expression reduced ER-mitochondria interactions and Ca^{2+} exchange and dampened hepatic insulin signaling and action, leading to fasting hyperglycemia in lean mice. The effect of FATE1 on membrane contact sites was rather specific to ER and mitochondria, as their interactions with LDs were not modified. However, it cannot be excluded that FATE1-mediated ER-mitochondria miscommunication impaired the activity of other organelles, as a consequence of mitochondria dysfunction. Furthermore, the moderate reduction (20%) in ER-mitochondria Ca^{2+} exchange induced by FATE1 was in agreement with the reduction observed in the early stages of HFHSD, confirming that a slight disruption of MAMs in the liver of lean mice is sufficient to reduce hepatic insulin sensitivity and to alter glucose homeostasis. Notably, these effects of FATE1 were independent of hepatic ER stress and not associated with hepatic inflammation or fibrosis. Interestingly, reinforcing organelle interactions and Ca^{2+} exchange by expressing an artificial linker prevented $HFHSD_{4W}$-induced glucose intolerance, confirming that preventing early diet-induced organelle miscommunication is sufficient to prevent metabolic alterations. Although we demonstrated a preventive effect of reinforcing MAMs on early-stage diet-induced metabolic alterations, our results contrast with those of another study showing that the linker worsens insulin resistance when expressed in mice already under a high-fat diet for several weeks.[11]

Our study further showed that ER-mitochondria miscommunication is not only causal but also reversible, since switching to SD for 8 weeks improved both organelle communication and hepatic insulin signaling and action in obese mouse liver. It is well known that food restriction is an effective strategy to improve glycemia in patients with T2D.[24] The present data showed that the improvement in systemic and hepatic insulin sensitivity required 8 weeks' RD, since improvement of obesity and glucose intolerance was observed only after 4 weeks. Interestingly, only RD_{8W} improved hepatic ER-mitochondria interactions (at least at structural levels, as we were not able to unequivocally assess MAM function in obese hepatocytes), again demonstrating that MAM structure is improved concomitantly with hepatic insulin sensitivity. However, these are merely

correlations, and it remains unclear whether improvement in MAMs contributes to or is a consequence of metabolic improvement. To investigate this, we expressed FATE1 in $HFHSD_{16W}$ mice before implementing RD_{8W}, in order to determine whether the beneficial effect of RD was linked to the improvement in ER-mitochondria interactions. Unfortunately, however, almost all the $HFSHD_{16W}$ mice infected with Ad-FATE1 (8/10) died a few days after the infection, whereas no mice infected with Ad-mCherry died (data not shown), and this prevented analysis of causality. These data highlight the detrimental effects of dampening ER-mitochondria interactions in a context of metabolic disease with liver injury.

Hepatic insulin resistance and steatosis are intimately connected in diet-induced obesity, and it is currently unknown which precedes and triggers the other.[25] Interestingly, mitofusin 2-related organelle miscommunication was recently associated with hepatic steatosis in non-alcoholic fatty liver disease.[9] Herein, we found that ER-mitochondria miscommunication preceded hepatic steatosis in mice with diet-induced obesity, and that FATE1-related disruption of ER-mitochondria interactions and Ca^{2+} exchange was sufficient to induce hepatic microsteatosis in lean mice, without hepatic inflammation and fibrosis. FATE1-related microsteatosis mainly implicates reduced mitochondrial oxidative capacity, involving both reduced mitochondrial lipid oxidation and alterations in mitochondrial bioenergetics. These mitochondrial alterations are likely linked to deficient ER-mitochondria calcium coupling, as both mitochondrial membrane potential and ROS production were not modified. In contrast, reinforcement of MAMs with the linker tended to increase lipid-related respiration and reduced the density of hepatic LDs, supporting a close relationship between MAM-related mitochondrial oxidative metabolism and hepatic lipid accumulation. Likewise, previous findings showed that ER-mitochondria coupling controlled mitochondrial respiration[26] and that autophagy-regulated fatty acid availability for oxidative phosphorylation involved MAMs.[27] Importantly, RD improved hepatic steatosis before organelle communication was reinforced and hepatic insulin sensitivity was improved, suggesting that this improvement is independent of MAMs and hepatic insulin sensitivity. It may also suggest that some intracellular lipids could influence organelle communication, impacting hepatic insulin sensitivity, and future lipidomic studies will be required to address this question. Importantly, an inverse relationship was on average observed between hepatic ER-mitochondria miscommunication and insulin sensitivity in obese patients with moderate hepatic steatosis. Despite the small size of the cohort, ER-mitochondria communication tended to decrease with steatosis severity ($p = 0.07$) only in diabetic patients (4 patients with mild steatosis (S1) *vs.* 7 with moderate or severe steatosis (S2-S3); data not shown). Therefore, additional studies with a larger number of patients are required to determine the link between MAMs and the severity of hepatic steatosis and MAFLD.

As ER-mitochondria miscommunication was also associated with skeletal muscle,[6] adipose tissue[28] and heart[29] insulin resistance, and with glucotoxicity-mediated β-cell dysfunction,[7] the present observations confirm the crucial role of MAMs in the control of glucose homeostasis and suggest that targeting MAMs may be a novel and effective strategy to improve whole-body metabolic homeostasis in MAFLD.

Abbreviations

ER, endoplasmic reticulum; FATE1, fetal and adult testis-expressed 1; FCCP, carbonylcyanide-4-trifluoromethoxyphenylhydrazone; HFHSD, high-fat and high-sucrose diet; IP3R1, inositol trisphosphate receptor 1; IR, insulin receptor; LD, lipid droplet; MAMs, mitochondria-associated membranes; PKB, protein kinase B; PLA, proximity ligation assay; PMHs, primary mouse hepatocytes; RD, reversal diet; ROS, reactive oxygen species; SD, standard diet; T2D, type 2 diabetes; TEM, transmission electronic microscopy; VDAC1, voltage-dependent anion channel 1.

Financial support

This study was supported by a research grant from both the Fondation de France (n°00056853) and the European Association for the Study of Diabetes (EFSD) to JR and from the Association Française pour l'Etude du Foie (AFEF) to PG. It was also funded by INSERM (France) and by the French National Research Agency (ANR) (#ANR-18-CE14-0019-02, #ANR-19-CE14-0044-01, #ANR-21-CE14-0015-03) and through the "Investments for the Future" LABEX SIGNALIFE (#ANR-11-LABX-0028-01) and the UCAJEDI Investments in the Future project (#ANR-15-IDEX-01). AB was supported by a research fellowship from the French Ministry of Higher Education and Research.

Conflict of interest

The authors have no conflicts of interest to disclose related to this study.

Please refer to the accompanying ICMJE disclosure forms for further details.

Authors' contributions

AB and JR designed the experiments, researched and analyzed data, contributed to the Discussion, and wrote the manuscript. MD, BP, MAB., JJ, CD, NB, SC, AVM, CCDS, LG and MP collected data. SP, RA, AI, AT and PG performed the clinical investigations and the sampling of liver biopsies of obese patients without or with type 2 diabetes. MP, LG and HV contributed to the Discussion and reviewed/re-edited the manuscript. JR is the guarantor of this work and, as such, had full access to all the data in the study and takes responsibility for the integrity of the data and the accuracy of the data analysis.

Data availability statement

All data are available upon reasonable request.

Acknowledgments

We thank Enzo Lalli (CNRS UMR7275, Valbonne, France) for the gift of FATE1 vectors; Gyorgi Hajnoczky and Gyorgi Csordas (Thomas Jefferson institute, Philadelphia, USA) for the generous gift of the ER-mitochondria linker and for sharing their macro to analyze ER-mitochondria interactions by TEM; Roger Tsien (University of California, San Diego, USA) for the generous gift of 4mtD3cpv vector; Elisabeth Errazuriz for her technical help at the CIQLE Imaging Center (Lyon, France); and Anaïs Alves (INSERM U1060, Lyon, France) for her occasional help with TEM analysis.

Supplementary data

Supplementary data to this article can be found online at https://doi.org/10.1016/j.jhep.2022.03.017.

References

[1] Theurey P, Rieusset J. Mitochondria-associated membranes response to nutrient availability and role in metabolic diseases. Trends Endocrinol Metab 2017;28:32–45.
[2] Wang J, He W, Tsai P, Chen P, Ye M, Guo J, et al. Mutual interaction between endoplasmic reticulum and mitochondria in nonalcoholic fatty liver disease. Lipids Health Dis 2020;19:72.
[3] Filadi R, Theurey P, Pizzo P. The endoplasmic reticulum-mitochondria coupling in health and disease: molecules, functions and significance. Cell Calcium 2017;62:1–15.
[4] Tubbs E, Theurey P, Vial G, Bendridi N, Bravard A, Chauvin MA, et al. Mitochondria-associated endoplasmic reticulum membrane (MAM) integrity is required for insulin signaling and is implicated in hepatic insulin resistance. Diabetes 2014;63:3279–3294.
[5] Theurey P, Tubbs E, Vial G, Jacquemetton J, Bendridi N, Chauvin M-A, et al. Mitochondria-associated endoplasmic reticulum membranes allow adaptation of mitochondrial metabolism to glucose availability in the liver. J Mol Cell Biol 2016;8:129–143.
[6] Tubbs E, Chanon S, Robert M, Bendridi N, Bidaux G, Chauvin M-A, et al. Disruption of mitochondria-associated endoplasmic reticulum membranes (MAMs) integrity contributes to muscle insulin resistance in mice and humans. Diabetes 2018;33:1–44.
[7] Dingreville F, Panthu B, Thivolet C, Ducreux S, Gouriou Y, Pesenti S, et al. Differential effect of glucose on ER-mitochondria Ca2+ exchange participates in insulin secretion and glucotoxicity-mediated dysfunction of β-cells. Diabetes 2019;68:1778–1794.
[8] Thivolet C, Vial G, Cassel R, Rieusset J, Madec A-M. Reduction of endoplasmic reticulum- mitochondria interactions in beta cells from patients with type 2 diabetes. PLoS One 2017;12:e0182027.
[9] Hernández-Alvarez MI, Sebastián D, Vives S, Ivanova S, Bartoccioni P, Kakimoto P, et al. Deficient endoplasmic reticulum-mitochondrial phosphatidylserine transfer causes liver disease. Cell 2019;177:881–895.e17.
[10] Anastasia I, Ilacqua N, Raimondi A, Lemieux P, Ghandehari-Alavijeh R, Faure G, et al. Mitochondria-rough-ER contacts in the liver regulate systemic lipid homeostasis. Cell Rep 2021;34:108873.
[11] Arruda AP, Pers BM, Parlakgül G, Güney E, Inouye K, Hotamisligil GS. Chronic enrichment of hepatic endoplasmic reticulum–mitochondria contact leads to mitochondrial dysfunction in obesity. Nat Med 2014;20:1427–1435.
[12] Thoudam T, Ha CM, Leem J, Chanda D, Park JS, Kim HJ, et al. PDK4 augments ER–mitochondria contact to dampen skeletal muscle insulin signaling during obesity. Diabetes 2019;68:571–586.
[13] Giacomello M, Pellegrini L. The coming of age of the mitochondria–ER contact: a matter of thickness. Cell Death Differ 2016;23:1417–1427.
[14] Townsend LK, Brunetta HS, Mori MAS. Mitochondria-associated ER membranes in glucose homeostasis and insulin resistance. Am J Physiol Metab 2020;319:E1053–E1060.
[15] Tubbs E, Rieusset J. Study of endoplasmic reticulum and mitochondria interactions by in situ proximity ligation assay in fixed cells. J Vis Exp 2016;2016.
[16] Rowland AA, Voeltz GK. Endoplasmic reticulum-mitochondria contacts: function of the junction. Nat Rev Mol Cell Biol 2012;13:607–615.
[17] Palmer AE, Giacomello M, Kortemme T, Hires SA, Lev-Ram V, Baker D, et al. Ca2+ indicators based on computationally redesigned calmodulin-peptide pairs. Chem Biol 2006;13:521–530.
[18] Doghman-Bouguerra M, Granatiero V, Sbiera S, Sbiera I, Lacas-Gervais S, Brau F, et al. FATE1 antagonizes calcium- and drug-induced apoptosis by uncoupling ER and mitochondria. EMBO Rep 2016;17:1264–1280.
[19] Csordás G, Várnai P, Golenár T, Roy S, Purkins G, Schneider TG, et al. Imaging interorganelle contacts and local calcium dynamics at the ER-mitochondrial interface. Mol Cell 2010;39:121–132.
[20] Rieusset J, Fauconnier J, Paillard M, Belaidi E, Tubbs E, Chauvin M-A, et al. Disruption of calcium transfer from ER to mitochondria links alterations of mitochondria-associated ER membrane integrity to hepatic insulin resistance. Diabetologia 2016;59:614–623.
[21] Vial G, Chauvin M-A, Bendridi N, Durand A, Meugnier E, Madec A-M, et al. Imeglimin normalizes glucose tolerance and insulin sensitivity and improves mitochondrial function in liver of a high-fat, high-sucrose diet mice model. Diabetes 2015;64:2254–2264.
[22] Garcia J, Decker CW, Sanchez SJ, Ouk JM, Siu KM, Han D. Obesity and steatosis promotes mitochondrial remodeling that enhances respiratory capacity in the liver of ob/ob mice. FEBS Lett 2018;592:916–927.
[23] Sebastián D, Hernández-Alvarez MI, Segalés J, Sorianello E, Muñoz JP, Sala D, et al. Mitofusin 2 (Mfn2) links mitochondrial and endoplasmic reticulum function with insulin signaling and is essential for normal glucose homeostasis. Proc Natl Acad Sci U S A 2012;109:5523–5528.
[24] Ley SH, Ardisson Korat AV, Sun Q, Tobias DK, Zhang C, Qi L, et al. Contribution of the Nurses' Health Studies to uncovering risk factors for type 2 diabetes: diet, lifestyle, biomarkers, and genetics. Am J Public Health 2016;106:1624–1630.
[25] Lockman KA, Nyirenda MJ. Interrelationships between hepatic fat and insulin resistance in non- alcoholic fatty liver disease. Curr Diabetes Rev 2010;6:341–347.
[26] Cárdenas C, Miller RA, Smith I, Bui T, Molgó J, Müller M, et al. Essential regulation of cell bioenergetics by constitutive InsP3 receptor Ca2+ transfer to mitochondria. Cell 2010;142:270–283.
[27] Bosc C, Broin N, Fanjul M, Saland E, Farge T, Courdy C, et al. Autophagy regulates fatty acid availability for oxidative phosphorylation through mitochondria-endoplasmic reticulum contact sites. Nat Commun 2020;11:4056.
[28] Wang CH, Chen YF, Wu CY, Wu PC, Huang YL, Kao CH, et al. Cisd2 modulates the differentiation and functioning of adipocytes by regulating intracellular Ca2+ homeostasis. Hum Mol Genet 2014;23:4770–4785.
[29] Dia M, Gomez L, Thibault H, Tessier N, Leon C, Chouabe C, et al. Reduced reticulum–mitochondria Ca2+ transfer is an early and reversible trigger of mitochondrial dysfunctions in diabetic cardiomyopathy. Basic Res Cardiol 2020;115:74.